ELSEVIER

Journal of Alloys and Compounds 235 (1996) 216–224

Journal of ALLOYS AND COMPOUNDS

Plutonium dioxide particle properties as a function of calcination temperature

Xavier Machuron-Mandard[a], Charles Madic[b]

[a]*Commissariat à l'Energie Atomique, INSTN, CE-Saclay, F-91191 Gif-sur-Yvette, France*
[b]*Commissariat à l'Energie Atomique, DCC-DRDD-SEMP, CEN-Fontenay-aux-Roses, F-92265 Fontenay-aux-Roses, France*

Received 12 August 1995; in final form 20 October 1995

Abstract

Powder samples of plutonium dioxide calcined at different temperatures have been characterized. Microcrystal size, number and mass distributions, particle morphology and specific surface area have been studied as a function of the oxide calcination temperature. Microcrystal sizes increase as a result of an increase in the calcination temperature; in contrast, the mass distribution of particle size is not very sensitive to this parameter. Even if not characterized directly, surface roughness and porosity are certainly decreasing functions of calcination temperatures since the grain surface structure and morphology, as well as the specific surface area, significantly decrease with increasing calcination temperatures.

Keywords: Plutonium dioxide; Plutonium oxalate; Calcination temperature; Powder sample characterization; Specific surface area

1. Introduction

In dealing with reprocessing of nuclear fuels or treatment of radioactive wastes from industry or laboratories, one of the problems to solve is solubilization of the actinide compounds present as oxides, which are more or less resistant to dissolution. Indeed, even if electrorefining in molten salts is reported as a possible method for treating particular fuels, [1–3] the processing of water-cooled reactor fuels and their resulting wastes is based mainly on hydrometallurgical concepts requiring preliminary dissolution of valuable elements (i.e. enriched uranium and transuranium elements) in acidic aqueous media [1,4–6]. Uranium and plutonium make up the major portion of the elements recovered, and the problem of actinide element recovery will become more acute with the increasing use of MOX-fuels in water reactors [7,8].

In contrast to uranium dioxide, plutonium dioxide is particularly resistant to dissolution in nitric acid medium. Consequently, various processes devoted to PuO_2 dissolution have been designed worldwide [9]. The classical industrial dissolution processes were based on the use of a boiling nitric–hydrofluoric acid medium in a corrosion-resistant system. Currently, the catalyzed electrolytic plutonium oxide dissolution concept (CEPOD) is being increasingly applied [10], which leads to flexible processes such as that of using dissolution of PuO_2 through oxidation by Ag(II) ions generated electrically in a nitric acid medium [11–14].

Since PuO_2 also dissolves readily by reduction, we have undertaken fundamental work dealing with the reductive dissolution of PuO_2 by Cr(II) ions generated electrically [15,16]. In addition to convenient reaction rates observed under the experimental conditions applied, Cr(II) has been selected as a reducing agent owing to its inner-sphere coordination properties, which enabled basic studies of the electron-transfer mechanism to be undertaken. Thus, our work includes both reaction mechanism and kinetics aspects.

Obviously, the detailed study of heterogeneous reactions involving both solid materials and ionic species in solution requires the perfect description of the reaction interface in terms of structure and reactivity [17]. However, the knowledge of this interface remains one of the most difficult points for such a study. Nevertheless, the reaction interface properties are thought to depend partly on the bulk solid material properties; consequently, the perfect characterization of the solid must be considered as essential for obtaining a better understanding of the interface reactivity [18].

SSDI 0925-8388(95)02122-1

Beyond crystal structure determination (i.e. lattice and microcrystal size, crystal face atom density), a knowledge of chemical purity and stoichiometry can be essential for technical reasons such as high-temperature deformation and material sintering properties, which are important for both fuel manufacture and storage. Moreover, it is fundamental, from an electronic viewpoint, since many materials have semiconductor properties. These electron properties can drastically change the interface behaviour, since the surface can act as an electron transfer site and as a catalyst [19]. Furthermore, the photochemical behaviour, or more generally speaking, the response of materials to irradiation, strongly depends on their electron band structure and is consequently very sensitive to the presence of impurities and stoichiometry defects [20]. Namely, the specific activity of radioactive materials that is responsible for very intense irradiation rates must be determined, which should always be achieved unambiguously by isotope composition measurements. Aside from electronic phenomena, adsorption often takes place at the solid interface. For solids in equilibrium with an aqueous solution, ion exchanges are observed as a result of acid–base properties [21]. The oxide's interface acts as a proton acceptor or donor, depending on the acidity or ionic content of the surrounding medium. According to classical concepts, this leads to aquo, hydroxo and oxo metallic sites (i.e. $M-OH_2^+$, M–OH and $M-O^-$ respectively) for which acidic constants can be defined and measured. The existence of such properties is of major interest, since coordination structures can appear at those sites and act as one of the first (and main) steps for subsequent chemical progress of the interface.

Besides intrinsic properties such as those mentioned above, the solids are usually available as powders consisting of particles having different shapes and sizes. The determination of these extrinsic properties (i.e. the resulting particle morphology) is also essential for the study of reaction rates [18]. Among those, the surface area, which is often a result of macro- and microporosity, determines the extent of the interface area. Consequently, both porosity and specific area are of major interest for kinetics studies. In fact, the development of fractal object theory should be an alternative means for studying the heterogeneous reaction rates [22]. Concerning the overall rates for isotropic heterogeneous reactions, however, the modelling of solid particles as objects having simple geometric shapes is required [23]. From that point of view, scanning electron microscopy and image analysis permit a better knowledge of particle morphology of powder materials to be gained, which is fundamental here. Moreover, this morphology model must be combined with particle size distribution functions resulting from particle size analysis, so as to precisely calculate the chemical reaction progress [23]. In addition, the particle size itself can be a major parameter determining particle hydrodynamic behaviour, which is very important for chemical reactor design; also, the size distribution can affect the powder material storage stability in term of size distribution homogeneity over long storage periods. Finally, it must be pointed out that the observation of the particle shape during the reaction progress, by sampling and analysis at different reaction times, can permit the detection of very interesting reaction aspects, such as particular corrosion routes or particle shape modification resulting from crystal face reactivity anisotropy. This can also be an interesting way of providing striking evidence of isotropic heterogeneous reaction mechanisms.

As illustrated above, the determination of powder material characteristics is an important but difficult task. In fact, these characteristics cannot be obtained easily since some of them require very special experimental devices not available in every laboratory. Consequently, this paper deals with some experiments we performed for characterizing PuO_2 batches used throughout our kinetics research [15,16]. Lattice and microcrystal sizes, morphology of particles, size distribution functions and specific surface areas are among the parameters obtained as function of the PuO_2 calcination temperature presented herein.

2. Results and discussion

2.1. Preparation of plutonium dioxide from plutonium(IV) oxalate

Except for plutonium, the chemicals used were all analytical grade reagents (Prolabo–R.P. Normapur). The aqueous solutions were prepared with high-grade distilled water. The plutonium used was supplied by the Commissariat à l'Energie Atomique (French Atomic Energy Commission) as plutonium dioxide, the form in which this element is stocked.

PuO_2 was dissolved in nitric acid solution by using Ag(II) ions as electrocatalyst; this leads to soluble Pu(VI) species [11]. After reduction of PuO_2^{2+} ions with hydrogen peroxide and destruction of the reducing agent excess by boiling of the solution, a pure Pu(IV) nitrate solution was obtained by purification through an anion exchange resin (i.e. Dowex 1-X2; Bio-rad) [24,25]. It must be pointed out that Pu(VI) oxalate can explode when heated during conversion into dioxide; therefore, total Pu(VI) reduction must be achieved and checked before Pu(IV) oxalate precipitation [26]. Testing of the radiochemical purity of the plutonium and of the elimination of americium 241

resulting from the β^- decay of ^{241}Pu was done by alpha spectrometry.

Plutonium oxalate was prepared after adjustment of the acidity of the solution ([Pu(IV)], 8 g l^{-1}; [HNO_3], 4 M). The oxalic acid, diluted in 0.5 l of 4 M nitric acid, was added slowly to the hot solution ($T = 50°C$) over a period of 1 h. Except for the addition of the two equivalents of oxalic acid required to precipitate the oxalate of plutonium (IV), the final concentration of this acid was fixed at 0.05 M to reduce the solubility of $Pu(C_2O_4)_2 \cdot 6H_2O$. The precipitate was subjected to another 1 h digestion period at 50°C. After cooling, it was filtered on ashless filter paper without washing.

The initial batch of PuO_2 was prepared by firing the Pu(IV) oxalate in air at 450°C for 5 h. Other samples of PuO_2 fired at different temperatures ranging from 450 to 1050°C, which all came from this initial batch, were subjected to calcination in air at the desired temperature in a silica crucible for 5 h. At the end of this time the crucible was immediately removed from the furnace and placed in open air in the glove box for rapid cooling of the oxide. The batches prepared in this manner were stored under dry nitrogen in hermetically sealed flasks to prevent adsorption of any gas or moisture at the surface of the PuO_2.

The plutonium isotopic composition was determined by thermoionization mass spectrometry. By combining these data with the plutonium isotope decay rates [27], the specific activity of PuO_2 is estimated to be 5×10^{12} Bq kg^{-1} (136 Ci kg^{-1}). It must be emphasized that 53.8% of this activity correspond to β^- emission due to ^{241}Pu, although the plutonium used was principally made of alpha-particle emitter isotopes (Table 1). Other nuclear events such as neutron emission resulting from α,n reactions (e.g. due to oxygen nuclei subjected to alpha particle radiations) were not taken into account.

Despite the importance of such characteristics, neither chemical purity nor oxygen stoichiometry could be determined in our laboratory. However, ion chromatography and the subsequent crystallization steps were validated many times over in the past and have been considered as certified procedures yielding high purity levels [24].

Stoichiometry, for its part, requires very accurate and difficult measurements [28–30]. For a comprehensive discussion about plutonium–oxygen compounds, we refer the reader to the review published by Cleveland [31]. Although there is no doubt about the existence of the sub-stoichiometric phases (i.e. PuO_{2-x}) [32], the existence of slightly super-stoichiometric plutonium dioxide (PuO_{2+x}) had not clearly been shown until recent work by Stakebake et al. [33] Indeed, according to Drummond and Welch [34] or Waterbury et al. [35], super-stoichiometric dioxides can be obtained under ordinary conditions by calcination of various plutonium compounds (e.g. sulphate, oxalate, hydroxide) in air. Contradicting the thermodynamic calculations of Brewer [36], who concluded that oxides higher than PuO_2 are probably unstable, these authors mentioned that the composition of the dioxide can be varied from $PuO_{2.0}$ to $PuO_{2.1}$, depending on the initial composition and the calcination temperature. They reported that a stoichiometric dioxide (i.e. $PuO_{2.002 \pm 0.008}$) can be obtained above 1200°C in certain cases, but the perfect stoichiometry cannot be attained from the Pu(IV) oxalate, even after 4 h of calcination at 1250°C, which leads to O/Pu ratios equal to 2.014 [35]. Other authors have mentioned the existence of excess oxygen dissolution in the lattice or superficial structures, resulting from the adsorption of oxygen, to explain an O/Pu ratio greater than 2 [32,37,38]. As noted above, Stakebake et al. [33] more recently reported the existence of gas–solid interface structures corresponding to the mixed-valence phase $Pu(IV)_{3-x}Pu(VI)_xO_{6+x}$ with $x \approx 0.5$ as a result of plutonium–water reactions under 15 Torr water vapour pressure between 200 and 350°C. From these data and all things considered, the stoichiometry of bulk plutonium dioxide can be dubious when the oxide is prepared by Pu(IV) oxalate calcination. Unfortunately, the technology required for obtaining reliable data about stoichiometry was not available in our laboratory, and therefore we did not determine the O/Pu ratio. Nevertheless, the plutonium dioxide we obtained should be very much like that resulting from plutonium oxalate calcined at 550°C in air, which has been reported to yield $PuO_{2.0 \pm 0.1}$ [39].

Table 1
Isotopic composition of the plutonium used

Plutonium isotope	Content (at.%)
^{238}Pu	0.0259
^{239}Pu	96.7090
^{240}Pu	3.0780
^{241}Pu	0.0798
^{242}Pu	0.1073

2.2. Crystallographic characteristics of plutonium dioxide

Three of the batches of the oxide studied were examined by X-ray crystallography using the well-known Debye–Scherrer method. The diffractograms were recorded using a copper-target X-ray tube and a Philips PW1020/20 Debye–Scherrer powder camera (360 mm circumference). All these PuO_2 batches were obtained by applying the experimental protocol described above and were calcined at 450, 550 and 1050°C. The diffraction patterns obtained allowed identification of the face-centred cubic structure that is natural for all actinide dioxides. The lattice parameter

a_0 corresponding to the distance between the (100) planes was measured. For each of the three samples analysed, the value obtained was (0.5396 ± 0.0004) nm. No significant difference was thus observed with the result generally accepted for ambient temperature (i.e. 0.53960 ± 0.00003 nm) [31,40,41].

By measuring the diffraction line width, the size of the crystallites making up the PuO_2 grains was estimated [42]. The determination of the size of these microcrystals was done on the PuO_2 samples calcined at 450 and 550°C. The oxide prepared at 1050°C was assumed to be crystalline enough to be used as a reference for taking into account the instrumental broadening of the lines caused by, among other things, the thickness of the sample-holding capillary (Table 2). Although the values obtained are not strictly identical to those reported in the literature, they are, nevertheless, of the same order of magnitude, confirming the work published by Kanellakopulos et al. [43] or Smith et al. [44]. In particular, they show the effect of broadening the microcrystalline zones under the influence of the thermal treatment at high temperature.

2.3. Particle size distribution analysis

As mentioned previously, and beyond the wish to characterize the material studied as well as possible, determination of the particle size distributions of various PuO_2 batches was achieved in order to obtain a representative mathematical function, which is very important to be able to model the dissolution kinetics curves. Theoretically speaking, both number or mass distributions of particle size can be used, but the mass distribution was selected and modelled owing to the more convenient mathematical treatment.

From an experimental point of view, the size distribution analyses were performed with a Coulter counter calibrated with a standard powder made of spherical grains 18.5 μm in diameter [45]. The samples were dispersed in an electrolytic solution but no preliminary reduction of any oxide powder aggregations (e.g. by sonication) was done. This protocol thus allowed an approach to the conditions in which our dissolution kinetics experiments were carried out.

Fig. 1 shows the number frequency distributions of PuO_2 calcined at different temperatures. The mass

Table 2
Influence of the calcination temperature of PuO_2 on the size of its crystallites

Calcination temperature (°C)	Size of the microcrystals (nm)		
	this work	Ref. [44]	Ref. [43]
450	190	80	100
550	320	100	200
1050	—	>1000	≈2000

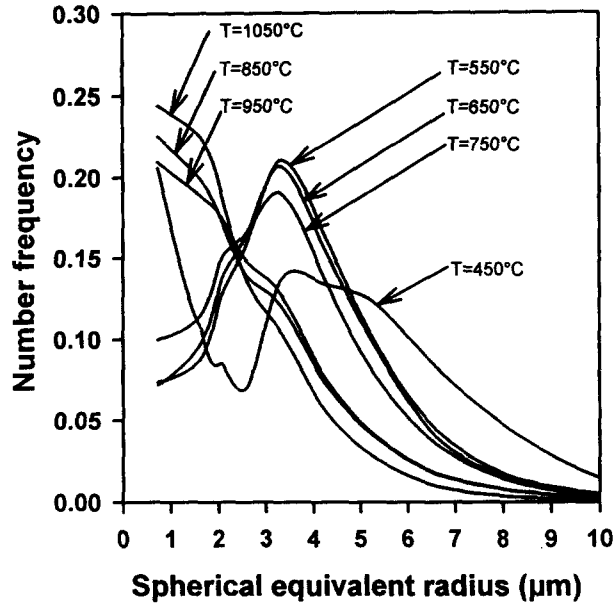

Fig. 1. Number frequency distributions for PuO_2 batches calcined at different temperatures (450–1050°C).

frequency histograms and their modelled functions are presented in Fig. 2. As is made clear by Fig. 1, two number distribution patterns were observed. Indeed, while the number of very small particles increases as the oxide is calcined at high temperature (i.e. above 750°C), the oxides fired at lower temperature are essentially made up of medium-sized grains. Only the oxide calcined at 450°C shows significant spreading of its distribution; unfortunately, no satisfactory explanation accounting for this spreading can be provided by us. Unlike the number distribution, and as shown in Fig. 2, the mass distributions are not very sensitive to the calcination temperature. This can be explained, at least in part, by assuming that rapid decrease in temperature at the end of the calcination can lead to grain surface crumbling or small grain splitting, which drastically increases the number of very small particles from a negligible oxide mass. Obviously, the thermal stress applied to the material is all the more violent and destructive as the calcination temperature is high.

Many mathematical models have been developed to represent correctly the particle size distribution of powder materials [45,46]. Log–normal analysis applied to the experimental distributions allowed representation of the size distributions $f(r)$ satisfactorily by a law expressed mathematically as follows [47,48]:

$$f(r) = \frac{1}{r\sigma(2\pi)^{1/2}} \exp\left\{-\frac{[\ln(r) - \mu]^2}{2\sigma^2}\right\} \quad (1)$$

where r is the radius of grains assumed to be spherical; μ and σ are the mean and standard deviation of $\ln(r)$ respectively. It must be pointed out that such a function satisfactorily fits with usual distributions

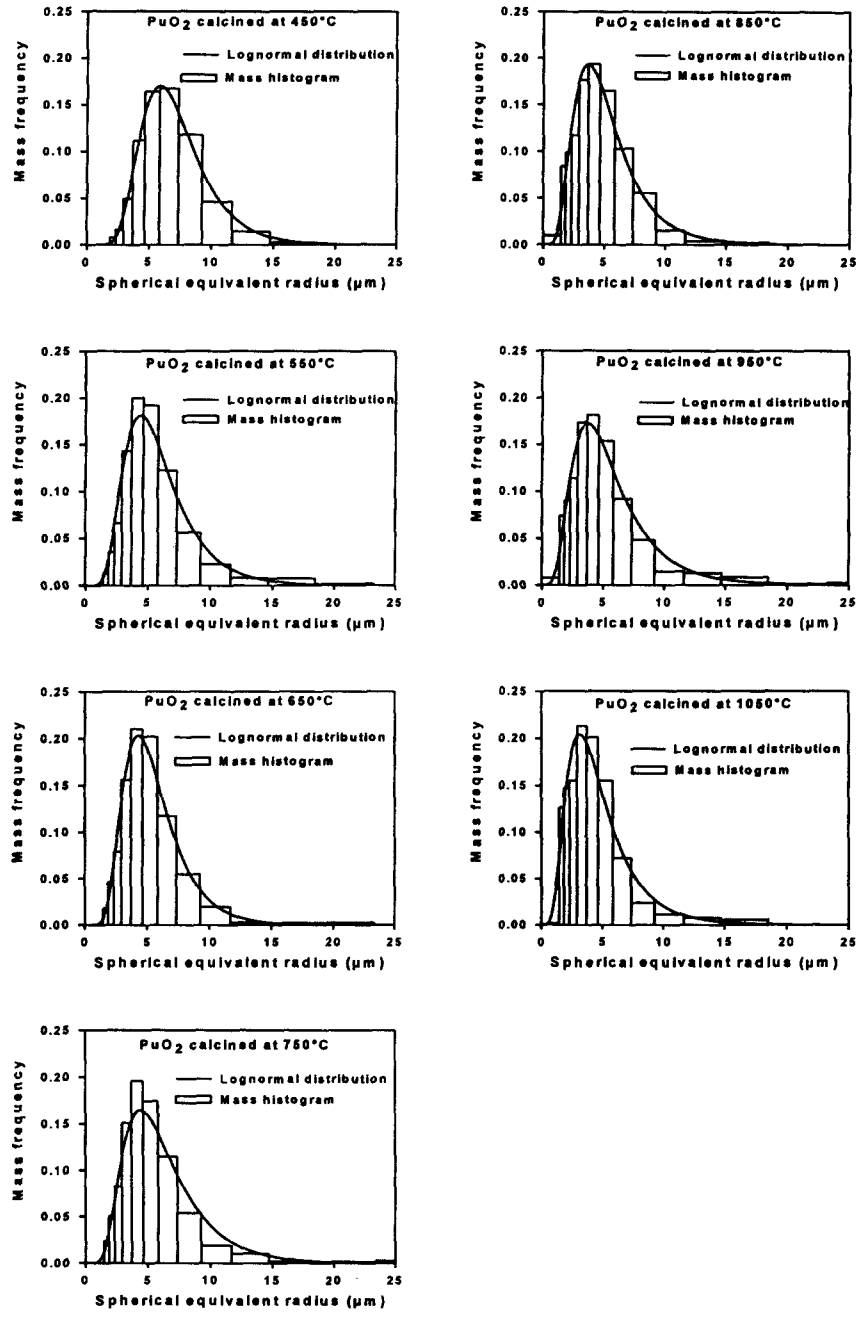

Fig. 2. Mass frequency histograms and log-normal distribution functions for PuO_2 batches calcined at different temperatures (450–1050°C).

skewed positively and verifies the relation of normalization expressed by

$$\lim_{r\to 0^+} \int_r^\infty f(r)\mathrm{d}r = 1 \qquad (2)$$

As mentioned above, in spite of the differences in calcination temperatures of the oxide batches, the particle size distributions presented in Fig. 2 are quite similar. This result seems to indicate that the size distribution by mass (or by volume, which is equivalent) of PuO_2 prepared by calcination of plutonium oxalate is not very sensitive to the thermal treatment undergone by the material. No growth in grain volume occurred during calcination, and the principal parameters of the particle size distribution (Table 3) for the oxide are certainly defined by those which the oxalate had, which depends on the physicochemical conditions of precipitation. No rupture of grains seemed to be observed. In contrast, however, if the mass of each grain remained constant, their shape and their porosity were subjected to important modifications, as can be clearly shown by microscopic examination of the PuO_2 powder.

Table 3
Log-normal distribution parameters as a function of the oxide calcination temperature

Calcination temperature (°C)	μ	σ
450	1.909	0.373
550	1.686	0.451
650	1.632	0.419
750	1.792	0.375
850	1.550	0.496
950	1.607	0.537
1050	1.432	0.540
Average value	1.658	0.456
Relative standard deviation (%)	8.8	14.4

2.4. Morphologic analysis of the grains of plutonium dioxide

As mentioned previously, like the particle size distribution function, the morphology of the oxide grains can be very important in development of a model of heterogeneous kinetics. The description of average grain morphology from statistical estimates is difficult, however, and requires the use of image analysis.

Nevertheless, observation of the sample by scanning electron microscopy (Leica-Stereoscan-100 encapsulated in a glove box) provided better understanding of the effect of the calcination temperature of PuO_2 on the value of its specific surface area. From the photographs presented in Fig. 3, it is clear that the powder samples are made up of two types of grain. Some show significant surface roughness and poorly defined shape (Fig. 3(A)). Others, smoother, correspond to truncated octahedra, which is consistent with the symmetry of the cubic system in which the actinide dioxides crystallize (Fig. 3(C)).

From the micrographs taken, we have logically observed that increase in the calcination temperature leads to increase in the proportion of smooth grains. This can be exemplified easily by comparing Fig. 3(A) with Fig. 3(B) obtained with PuO_2 calcined at 550°C and 750°C respectively.

The geometry of the grains obtained obviously depends on the synthesis procedure. Indeed, microscopic observations of actinide dioxides have often been made in syntheses of monocrystals having well-developed {100} or {111} faces [49–52]. In the case of PuO_2, the crystals obtained by slow crystallization in molten salts (e.g. $Li_2O.2MoO_3$) were reported to have octahedral shapes [52]. Our synthesis of PuO_2 by thermal decomposition of tetravalent plutonium oxalate did not produce crystals other than the irregular ones and the truncated octahedra. No cubic crystal was observed. Our results are not inconsistent with those published by Rankin and Burney [53], who reported the existence of spherical aggregates as a

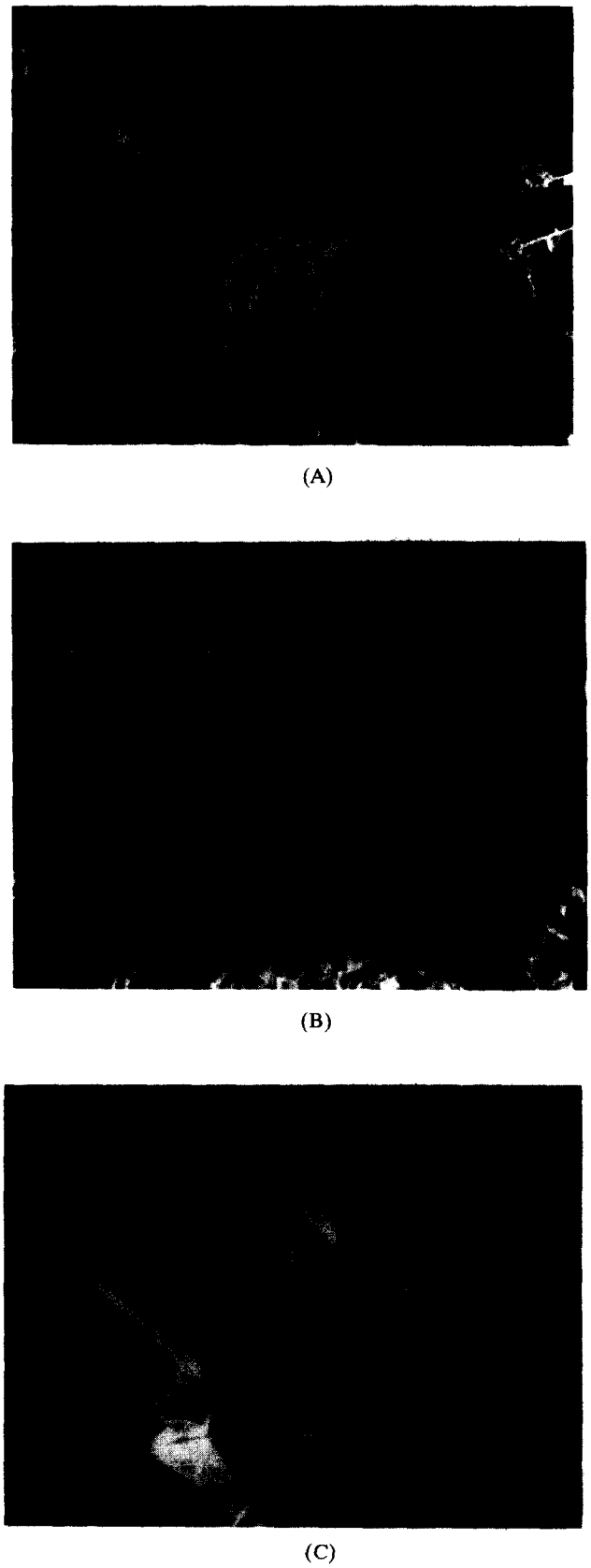

(A)

(B)

(C)

Fig. 3. Scanning electron microscope observations of PuO_2 particles. (A) PuO_2 calcined at 550°C forming mainly irregular grains. (B) PuO_2 calcined at 750°C having higher proportion of smooth grains. (C) PuO_2 calcined at 750°C allowing observation of specific morphology (truncated octahedra) of certain grains.

result of plutonium oxalate calcination between 450 and 700°C. Indeed, as mentioned above, particles having well-defined shapes are more easily observed for materials calcined at high temperatures (i.e. above 750°C). No information concerning the calcination duration, which is obviously among the major parameters contributing to change in particle shape due to atom motion, was provided by these authors. Moreover, because of the limited resolution of their optical microscope, the observation of small octahedral grains was probably impossible.

2.5. Specific surface area of plutonium dioxide

Among the principal characteristics of powders, the specific area is one of the most frequently determined. It effectively carries the meaning of the reaction interface and thus the reactivity of the material, which justifies its importance.

The specific surface area was obtained by dynamic measurement of nitrogen adsorption at −196°C (liquid nitrogen) using helium as carrier gas according to the B.E.T. method [54,55] The instrument used was the Quantasorb from Quantasorb Corp. connected to a thermal conductivity detector (i.e. katharometer) calibrated by pure nitrogen injections.

Fig. 4 summarizes the results obtained and shows the significant decrease in the value of the specific area when the calcination temperature of the oxide is increased. In agreement with the observations made from the microscope photographs, this result confirms the crystalline rearrangement that occurs at high temperatures, leading to the disappearance of the pores and of the crystalline irregularities at the surface

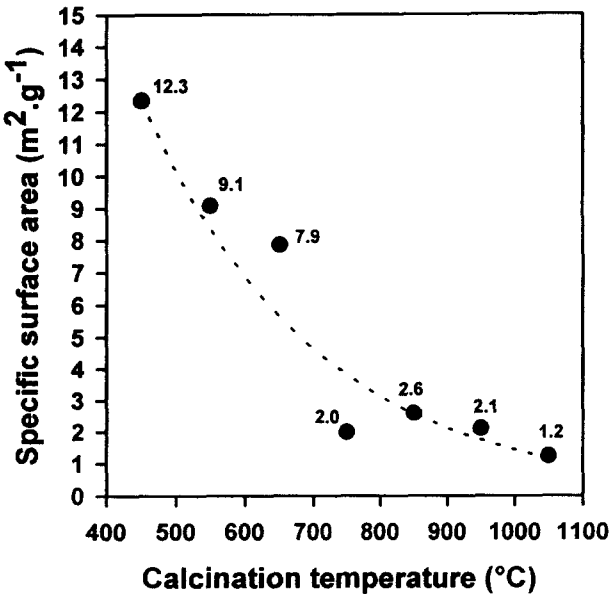

Fig. 4. Effect of the calcination temperature of PuO_2 on its B.E.T. specific surface area measured by nitrogen adsorption.

of the grains. This phenomenon probably extends to the complete mass of the crystal, which leads to a more compact internal structure and less superficial roughness as the temperature of calcination of the oxide increases. Although no empirical equation is proposed to take this phenomenon into account, Fig. 4 shows the quasi-exponential decrease of the specific surface as the calcination temperature increases. It must be pointed out that the values measured are similar to those usually published [56], but are far higher than those expected from theoretical estimates. Indeed, specific surface areas calculated from the experimental size distributions on the assumption of spherical grains should range from 0.05 to 0.9 $m^2\ g^{-1}$ (estimates calculated for PuO_2 calcined at 550°C and 1050°C respectively). The discrepancy between these estimates and the actual values, illustrates the major contribution of surface roughness and porosity to the surface area. Unfortunately, no study of the grain porosity was undertaken, although this would have allowed us to provide valuable information about the grain structure.

3. Conclusion

As previously mentioned, but paradoxically, few of the various characteristics presented in the Introduction were actually studied since their determination required many techniques not available in our laboratory. Moreover, the characterization of highly radioactive compounds obviously suffers from safety requirements, which made interlaboratory collaborations much more difficult.

However, the results presented herein held the key to our better understanding of the heterogeneous reductive dissolution of PuO_2 [15]. Although qualitative and quantitative information about metallic sites existing at the oxide–solution interface were missing, we provided undisputed evidence by using isotope labelling experiments that heterogeneous plutonium–oxygen structures are involved in the oxide dissolution mechanism by Cr(II) ions [15]. Similarly, but from kinetics experiments, Agarande showed that the PuO_2 dissolution by Ti(III) ions in sulphuric acid medium probably begins with the formation of non-uniform heterogeneous structures [57].

Such results illustrate the great importance of the interface properties for better understanding of the reactivity of PuO_2 and, more generally speaking, for understanding the reactivity of solids. Therefore, and beyond the study presented above, it must be emphasized that solid material dissolution and corrosion reactions are among the chemical phenomena having major importance for both basic understanding of matter reactivity and industrial applications. The in-

fluence of the non-solid phase properties (e.g. liquid or gaseous phase composition) on such reactions is usually tested first, since those properties can be varied more easily than those of the solid material. However, as mentioned in the introductory section of this paper, the solid phase characteristics can play a major role in the mechanism of a chemical action and, therefore, the characterization of solids should not be neglected whenever possible. The stimulation of collaborations between physicists mastering powerful characterization techniques and chemists in charge of studying heterogeneous chemical events is obviously the key to progress in this field.

Acknowledgements

The authors are grateful to Ms. Catherine Cossonnet, Mr. Jean Livet and Mr. Philippe Parmentier for their expert technical assistance.

References

[1] J.T. Long, *Engineering for Nuclear Fuel Reprocessing*, American Nuclear Society, La Grange Park, 1978, pp. 273–325.

[2] J.E. Battles, W.E. Miller and E.C. Gay, Pyrometallurgical processing of integral fast reactor metal fuels, *Proc. 3rd Int. Conf. Nuclear Fuel Reprocessing and Waste Management, RECOD'91, Sendai, Japan, April 14–18, 1991*, Vol. I, pp. 342–347.

[3] T. Kobayashi and M. Tokiwai, Development of TRAIL, a simulation code for the molten salt electrorefining of spent nuclear fuel, *J. Alloys Comp., 197* (1993) 7.

[4] R.E. Blanco and C.D. Watson, Head-end processes for solid fuels, in S.M. Stoller and R.B. Richards (eds.), *Reactor Handbook*, vol. II, *Fuel Reprocessing*, Interscience, New York, 1961, pp. 23–106.

[5] J. Sauteron, *Les Combustibles Nucléaires*, Hermann, Paris, 1965, pp. 337–415.

[6] E. Henrich, Chemie der PUREX-Eingangsstufe, in F. Baumgärtner (ed.), *Chemie der Nuklearen Entsorgung*, Teil III, Karl Thiemig, Munich, 1980, pp. 85–109.

[7] A. Bekiarian and G. Le Bastard, MOX manufacturing perspectives in a fast growing future and the MELOX plant, *Proc. 3rd Int. Conf. Nuclear Fuel Reprocessing and Waste Management, RECOD'91, Sendai, Japan, April 14–18, 1991*, Vol. I, pp. 201–206.

[8] W. Fournier and G. Dalverny, Le combustible MOX et l'usine de fabrication Melox, *Rev. Gen. Nucl., 1* (1995) 34.

[9] J.L. Ryan and L.A. Bray, Dissolution of plutonium dioxide—a critical review, in J.D. Navratil and W.W. Schulz (eds.), *Actinide Separations*, ACS Symp. Ser. 117, American Chemical Society, Washington, DC, 1980, pp. 499–514.

[10] J.L. Ryan, L.A. Bray, E.J. Wheelwright and G.H. Bryan, Catalyzed electrolytic plutonium oxide dissolution, in L.R. Morss and J. Fuger (eds.), *Transuranium Elements, a Half Century*, American Chemical Society, Washington, DC, 1992, pp. 288–304.

[11] J. Bourges, C. Madic, G. Koehly and M. Lecomte, Dissolution du bioxyde de plutonium en milieu nitrique par l'argent(II) électrogénéré, *J. Less-Common Met., 122* (1986) 303.

[12] C. Madic, M. Lecomte, J. Bourges, G. Koehly and J.P. Moulin, Mechanism of the rapid dissolution of PuO_2 under oxidizing conditions, and applications, *Proc. 3rd Int. Conf. Nuclear Fuel Reprocessing and Waste Management, RECOD'91, Sendai, Japan, April 14–18, 1991*, Vol. II, pp. 715–720.

[13] Y. Zundelevich, The mediated electrochemical dissolution of plutonium oxide: kinetics and mechanism, *J. Alloys Comp., 182* (1992) 115.

[14] F.J. Poncelet, M.H. Mouliney, V. Decobert and M. Lecomte, Industrial use of electrogenerated Ag(II) for PuO_2 dissolution, *Proc. 4th Int. Conf. Nuclear Fuel Reprocessing and Waste Management, RECOD'94, London, UK, April 24–28, 1994*, Vol. II.

[15] X. Machuron-Mandard, Etude de la cinétique et du mécanisme de la réaction de dissolution du bioxyde de plutonium par l'ion Cr(II) en solution acide, *Ph.D. Thesis*, Pierre and Marie Curie University, Paris VI, 1991.

[16] X. Machuron-Mandard and C. Madic, Basic studies on the kinetics and mechanism of the rapid dissolution reaction of plutonium dioxide under reducing conditions in acidic media, *J. Alloys Comp., 213–214* (1994) 100.

[17] A. Zangwill, *Physics at Surfaces*, Cambridge University Press, Cambridge, UK, 1990.

[18] P. Barret, *Cinétique Hétérogène*, Gauthier-Villars, Paris, 1973, pp. 84–96.

[19] Th. Wolkenstein, *Théorie Electronique de la Catalyse sur les Semi-Conducteurs*, Masson, Paris, 1961.

[20] V. Barou and Th. Wolkenstein, *Effet de l'Irradiation sur les Propriétés des Semi-Conducteurs*, Mir Publications, Moscow, 1982.

[21] J.P. Jolivet, *De la Solution à l'Oxyde*, InterEditions-CNRS Editions, Paris, 1994, pp. 255–308; 343–383.

[22] B. Mandelbrot, *Les Objets Fractals*, Flammarion, Paris, 1989.

[23] B. Delmon, *Introduction à la Cinétique Hétérogène*, Technip, Paris, 1969.

[24] J.M. Cleveland, Solution chemistry of plutonium, in O.J. Wick (ed.), *Plutonium Handbook—A Guide to the Technology*, Vols. I&II, American Nuclear Society, La Grange Park, 1980, pp. 456–463.

[25] J.J. Katz, G.T. Seaborg and L.R. Morss, *The Chemistry of Actinide Elements*, Chapman-Hall, London, 1986, pp. 550–569.

[26] J.M. Cleveland, Compounds of plutonium, in O.J. Wick (ed.), *Plutonium Handbook—A Guide to the Technology*, Vols. I&II, American Nuclear Society, La Grange Park, 1980, p. 374.

[27] DAMRI, *Radionucléides*, Commissariat à l'Energie Atomique-DAMRI, Saclay, 1991.

[28] M. Ganivet and A. Benhamou, Comparaison de deux méthodes de détermination du rapport oxygène-métal dans les oxydes mixtes d'uranium et de plutonium, in *Analytical Methods in the Nuclear Fuel Cycle, IAEA Symp. Proc., Vienna, November 29–December 3, 1971*, Rep. IAEA-SM-149/51, 1972, pp. 23–33.

[29] F. Toci, F.T. Ewart and M. Cambini, Determination of oxygen potentials and O/M ratios of oxide nuclear reactor fuels by means of an automated solid state galvanic cell, *Rep. EUR 10948 EN*, 1987 (Commission of the European Communities—JRC Ispra).

[30] G. Mühling, Stoichiometry in nuclear fuel oxides, *Rep. IGC-121 C*, 1991, pp. 50–57 (Indira Gandhi Centre for Atomic Research, Kalpakkam).

[31] J.M. Cleveland, Compounds of plutonium, in O.J. Wick (ed.), *Plutonium Handbook—A Guide to the Technology*, Vols. I&II, American Nuclear Society, La Grange Park, 1980, pp. 339–345.

[32] T.D. Chikalla, C.E. McNeilly and R.E. Skavdahl, The plutonium–oxygen system, *J. Nucl. Mater., 12* (1964) 131.

[33] J.L. Stakebake, D.T. Larson and J.M. Haschke, Characterization of the plutonium–water reaction, II: Formation of a binary oxide containing Pu(VI), *J. Alloys Comp., 202* (1993) 251.

[34] J.L. Drummond and G.A. Welch, The preparation and properties of some plutonium compounds. Part VI. Plutonium dioxide, *J. Chem. Soc.*, (1957) 4781.
[35] G.R. Waterbury, R.M. Douglass and C.F. Metz, Thermogravimetric behavior of plutonium metal, nitrate, sulfate, and oxalate, *Anal. Chem., 33* (1961) 1018.
[36] L. Brewer, The thermodynamic properties of the oxides and their vaporization processes, *Chem. Rev., 52* (1953) 1.
[37] E.E. Jackson and M.H. Rand, The oxidation behaviour of plutonium dioxide and solid solutions containing plutonium dioxide, *Rep. AERE-R-3636*, 1963 (United Kingdom Atomic Energy Authority, Harwell, UK).
[38] J.L. Stakebake and M.R. Dringman, Adsorption of oxygen on sintered plutonium dioxide, *J. Nucl. Mater., 23* (1967) 349.
[39] V.K. Rao, I.C. Pius, M. Subbarao, A. Chinnusamy and P.R. Natarajan, Precipitation of plutonium oxalate from homogeneous solutions, *J. Radioanal. Nucl. Chem., 100* (1986) 12.
[40] W.H. Zachariasen, *Nat. Nucl. Energ. Serv. Div. IV, 14* (1949) B-1442; B-1489.
[41] J.J. Katz, G.T. Seaborg and L.R. Morss, *The Chemistry of Actinide Elements*, Chapman–Hall, London, 1986, pp. 680–690.
[42] A. Guinier, *Théorie et Technique de la Radiocristallographie*, Dunod, Paris, 1956, pp. 462–489.
[43] B. Kanellakopulos, E. Dornberger, J. Müller, F. Baumgärtner, U. Benedict and D. Dufour, Über die Löslichkeit von Plutoniumdioxid in Salpetersäure, *Rep. KfK 3353-EUR 7989d*, 1983 (Kernforschungszentrum Karlsruhe).
[44] P.K. Smith, G.A. Burney, D.T. Rankin, D.F. Bickford and R.D. Sisson, Jr., Effect of oxalate precipitation on PuO_2 microstructures, *Rep. DP-MS-76-34*, 1976 (Dupont de Nemours).
[45] T. Allen, *Analyse Chimique et Caractérisations-Granulométrie*, Techniques del'Ingénieur, Paris, 1988, p. 1040.
[46] W.F. Tanner, C. Christiansen, D. Hartmann, J.P.M. Syvitski, S. Sengupta, J.K. Ghosh and B.S. Mazumder, Data interpretation and manipulation, in J.P.M. Syvitski (ed.), *Principles, Methods, and Application of Particle Size Analysis*, Cambridge University Press, Cambridge, UK, 1991, pp. 223–279.
[47] M. Moreau and A. Mathieu, *Statistique Appliquée à l'Expérimentation*, Eyrolles, Paris, 1979, pp. 95–96.
[48] D.B. Siano, The log–normal distribution function, *J. Chem. Educ., 49* (1972) 755.
[49] W. Müller and J.C. Spirlet, Progrès récents en croissance cristalline des actinides et de leurs composés, *Rev. Chim. Miner., 20* (1983) 786.
[50] J.C. Spirlet and O. Vogt, Sample preparation and crystal growth for solid state actinide research, in A.J. Freeman and G.H. Lander, *Handbook on the Physics and Chemistry of the Actinides*, Elsevier, 1984, pp. 79–151.
[51] J.C. Spirlet, W. Müller and J. van Audenhove, Single crystal growth of actinide compounds, *Nucl. Instr. Methods Phys. Res. A, 236* (1985) 489.
[52] C.B. Finch and G.W. Clark, High-temperature solution growth of single-crystal plutonium dioxide, *J. Cryst. Growth, 12* (1972) 181.
[53] D.T. Rankin and G.A. Burney, Particle size of $^{238}PuO_2$ obtained by oxalate precipitation and calcination, *Ceram. Bull., 54* (1975) 1061.
[54] J.H. de Boer, The BET-method, in D.H. Everett and R.H. Ottewill (eds.), *Surface Area Determination*, Butterworths, London, 1970, pp. 7–24.
[55] J. Charpin and B. Rasneur, *Analyse Chimique et Caractérisations-Mesure des Surfaces Spécifiques*, Techniques de l'Ingénieur, Paris, 1982, p. 1045.
[56] J. Edwards, G.R. Chilton, J.R. Stanbridge and W. Baxter, The conversion of plutonium into thermal reactor MOX fuel in the UK, *Proc. 3rd Int. Conf. Nuclear Fuel Reprocessing and Waste Management, RECOD'91, Sendai, Japan, April 14–18, 1991*, Vol. I, pp. 207–212.
[57] M. Agarande, Lixiviation de déchets solides plutonifères par des solutions de réducteurs électrogénérés, *Rep. CEA-R-5597*, 1992 (Commissariat à l'Energie Atomique).